

Dependence of Localized Deformation on Point Defect Development Caused by Intersected Cross Slip among Dislocations

Michiaki KOBAYASHI^{1,a}, Naohiro AOYAMA², Shou HASHIBA^{2,b}, Setsuo MIURA^{1,c} and
Jun-ichi SHIBANO^{1,d}

¹⁾ Department of Mechanical Engineering, Kitami Institute of Technology
Kitami, Hokkaido, 090-8507 JAPAN

²⁾ Graduate School of Kitami Institute of Technology
Kitami, Hokkaido, 090-8507 JAPAN

^{a)} kobayasi@mail.kitami-it.ac.jp, ^{b)} mme05014@std.kitami-it.ac.jp,
^{c)} miurast@mail.kitami-it.ac.jp, ^{d)} jshibano@mail.kitami-it.ac.jp

Keywords: Point defect, Elastic stiffness degradation, Criterion, Localized/diffused necking

Abstract. In this paper, via experimental results of ultrasonic wave velocity changes and FEM simulations of slip system under the pure shear plastic deformation of a pure Aluminum single crystal, the authors verify that the ultrasonic longitudinal wave velocity depends upon the development of point defects caused by intersected cross slip among dislocations and also examine the correlation of the point defect dependence of the longitudinal wave velocity with the elastic stiffness degradation due to plastic deformation damage which is closely related to the deformation instability mechanism.

Introduction

In the authors' previous studies [1]-[5], the dependence of ultrasonic wave velocity on the micro-structural property changes of solid materials under plastic deformation were investigated both theoretically and experimentally. For example it is found that longitudinal wave velocity changes between under the simple and pure shear states are quite different, on the other hand transverse wave velocity changes under simple and pure shear states are almost same as similar to the texture development under both shear states. These results clearly suggest that the propagating character of ultrasonic waves is dependent upon its interaction between the propagating mode of ultrasonic waves and micro-structural material changes induced by damage due to plastic deformation

Then the point defect dependence of the longitudinal wave velocity under the pure shear state is examined based on both of no point defects caused by intersected cross slip among dislocations under single slip stage simulated by finite element polycrystal model (FEM) analysis [6], [7] for crystal plasticity and experimental evidence of no longitudinal wave velocity changes under the same stage in a pure Aluminum single crystal.

The point defect dependence of the longitudinal wave velocity suggests the elastic stiffness degradation due to plastic deformation damage which is closely related to the deformation instability mechanism. Therefore, in this paper FEM numerical simulations regarding to the contour line of amount of point defects estimated by the calculation of the intersected cross slip among dislocations under several proportional loading paths are performed and compared with the experimental results of necking onset strains in an Aluminum specimen measured by laser speckle method. The good agreement between the simulated and experimental results regarding the onset of the deformation instability suggests that the proposed algorithm to calculate the amount of point defects caused by intersected cross slip among dislocations has ability to be unified criterion for both localized and diffused necking.

Longitudinal Wave Velocity Derived by Proposed Theoretical Model [2], [3]

One of authors formulated the ultrasonic wave velocities under plastic deformation and proposed the ultrasonic nondestructive material evaluation method. Then successively the authors evaluated

microstructural material property changes under plastic deformation via numerical simulations and experimental verifications. The formula of the longitudinal wave velocity derived by the proposed theoretical model is consisted with the physical nonlinearity so called acousto-elastic effect, the geometrical nonlinearity and the deformation induced anisotropy due to the elasto-plastic coupling effect as follows:

$$\rho_0 \mathbf{V}_L^2 = \lambda + 2\mathbf{G} - \frac{4}{9}\mathbf{G}^2(\lambda_{11}^c + \lambda_{22}^c) - \frac{16}{9}\mathbf{G}^2\lambda_{33}^c + \{1 - 4\mathbf{G}(3\lambda + 2\mathbf{G})(\kappa_2 + \frac{2}{3}\kappa_3) - \frac{8}{3}\mathbf{G}^2\kappa_3\}\sigma_3 - \frac{1}{3}\{(3\lambda + 2\mathbf{G})^2(6\kappa_1 + 3\kappa_2 + \frac{2}{3}\kappa_3) - 4\mathbf{G}\lambda(3\kappa_2 + 2\kappa_3) - \frac{8}{3}\mathbf{G}^2\kappa_3\}(\sigma_1 + \sigma_2 + \sigma_3) + 4(\lambda + 2\mathbf{G})(\epsilon_3^e + [\epsilon_3^p]) \quad (1)$$

In the shear states, the stress and strain components in out of plane and the sum of principal stresses in plane are zero, therefore the longitudinal wave velocity is deduced to be only dependent on the deformation induced anisotropy as follows:

$$\rho_0 \mathbf{V}_L^2 = \lambda + 2\mathbf{G} - \frac{4}{9}\mathbf{G}^2(\lambda_{11}^c + \lambda_{22}^c) - \frac{16}{9}\mathbf{G}^2\lambda_{33}^c \quad (2)$$

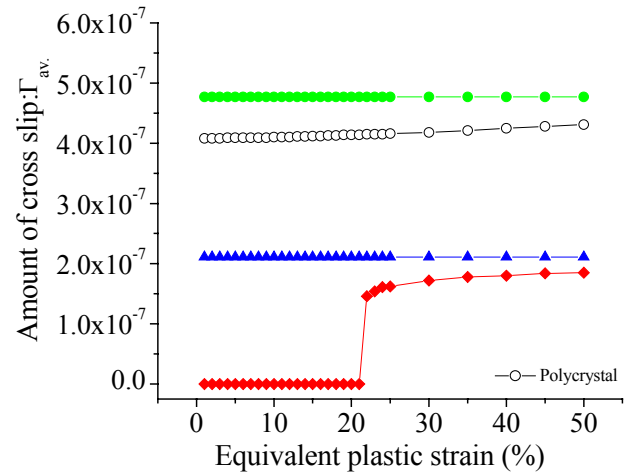
in which λ_{11}^c , λ_{22}^c and λ_{33}^c are zero under simple shear state theoretically, on the other hand are not zero under pure shear state, because λ_{ii}^c is dependent on normal plastic strains. Therefore, it was suggested theroretically and also verified experimentally [4] that the longitudinal wave velocity doesn't change under the simple shear plastic deformation and changes under the pure shear plastic deformation.

Definition of Intersected Cross Slip among Dislocations to Estimate Point Defects Density

It is well known that point defects caused by radiation damages influence on the ultrasonic wave velocity and jog motions of dislocations due to intersected slides such as cross slip under plastic deformation induce point defects. However, the direct calculation of point defects is extremely difficult now. Therefore, instead of the direct calculation of point defects, we calculate the multiplicative amount of intersected slides between primary and secondary slip systems, and then we use it to predict the induced possibility of point defects under pure shear state. It is well known that there are 12 slip systems in a crystal of FCC metals. Provided that one slip system among 12 slip systems is selected as a primary slip system, then there may exist 8 secondary slip systems crossing with the primary slip system. Here, we denote the slip amounts of primary slip system in crystal i as $\dot{\gamma}_i^p$ ($i=1\sim n$, $n=729$: number of FEM elements), and slip amounts of secondary slip systems crossing with the primary slip system in the same crystal i as $\dot{\gamma}_i^s$ ($s=1\sim 8$); then the multiplicative amounts Γ of intersected slides between primary and secondary slip systems is defined as [4]

$$\Gamma = n\Gamma_{av.} = \sum_{i=1}^n \sum_{s=1}^8 \dot{\gamma}_i^p \dot{\gamma}_i^s \quad (3)$$

in which $\Gamma_{av.}$ is average of Γ per element. The calculated results of $\Gamma_{av.}$ are shown in Fig.1 with comparison of 3 types of single crystals characterized by the crystal orientation as indicated by the standard stereo triangle in Fig.2 and the polycrystal case. And also as regarding with necking onset strains due to deformation instability



Crystal orientation	Euler angle [radian]		
	ϕ	θ	ψ
Type I —◆—	1.571	0.393	2.356
Type II —▲—	1.571	0.000	3.142
Type III —●—	1.571	5.498	3.142

Fig.1 Intersected cross slips among dislocation in various types of crystal orientation

Fig.3 indicates FEM numerically simulated contour line of amount of point defects estimated by Eq.(3) for polycrystal Aluminum under several proportional loading paths.

Experimental Verification of Point Defect Dependence of Longitudinal Wave Velocity

The block diagram of biaxial combined loading experimental setup in Fig. 4 is adopted to measure the flight time of the longitudinal wave propagating poly and single pure Aluminum specimens under pure shear plastic deformation.

Figure 5 shows the experimental results of longitudinal wave velocity under pure shear state of single and poly crystal. As seen from Fig.5, the magnitudes of the longitudinal wave velocity changes are in order of amount of point defects as shown in Fig.1; the longitudinal wave velocity in the case of crystal orientation type I doesn't change in the single slip stage and gradually decreases in the multi-slip stage. From the point defect dependence of the longitudinal wave velocity to be closely related to the elastic stiffness, it is suggested that the amount of point defects causes the elastic stiffness degradation and then it induces the deformation instability. Therefore, the proposed algorithm defined by Eq.(3) to calculate the amount of point defects caused by intersected cross slip among dislocations has ability to be unified criterion for both localized and diffused necking.

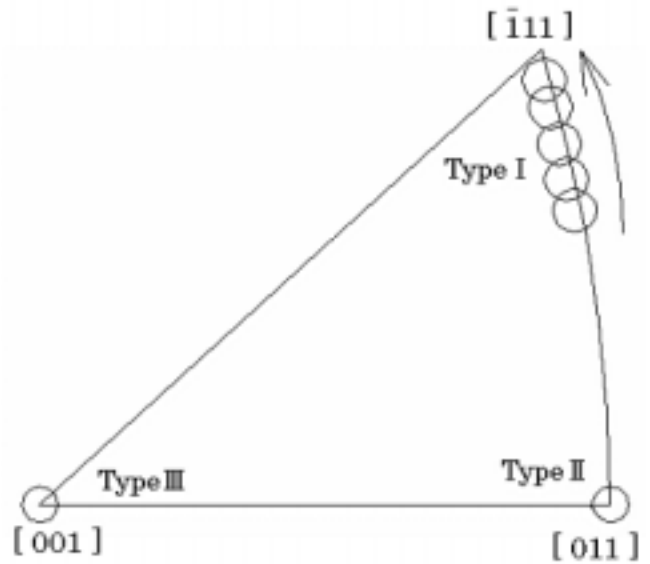


Fig.2 Shear stress direction in standard stereo triangle under pure shear state

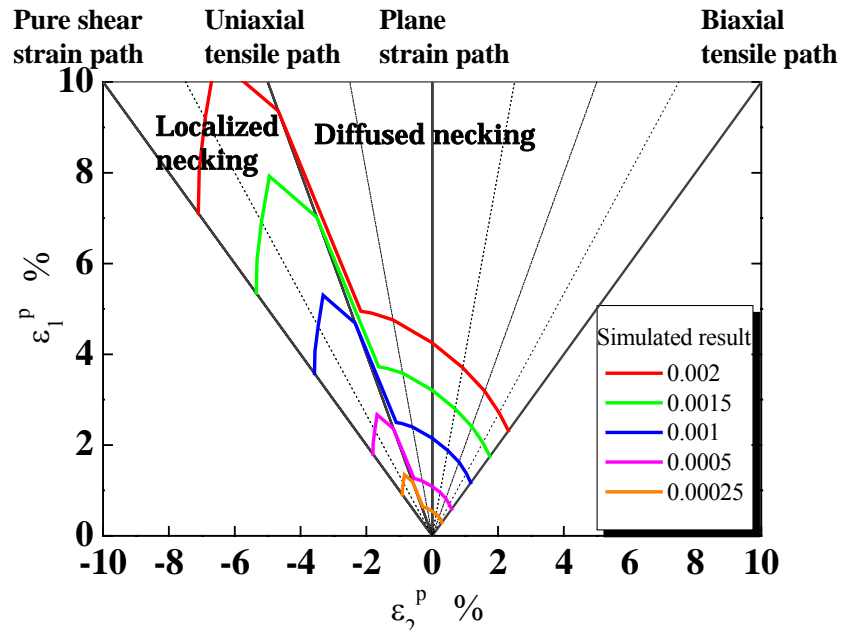


Fig.3 Contour lines of the integrated Γ under proportional loading paths

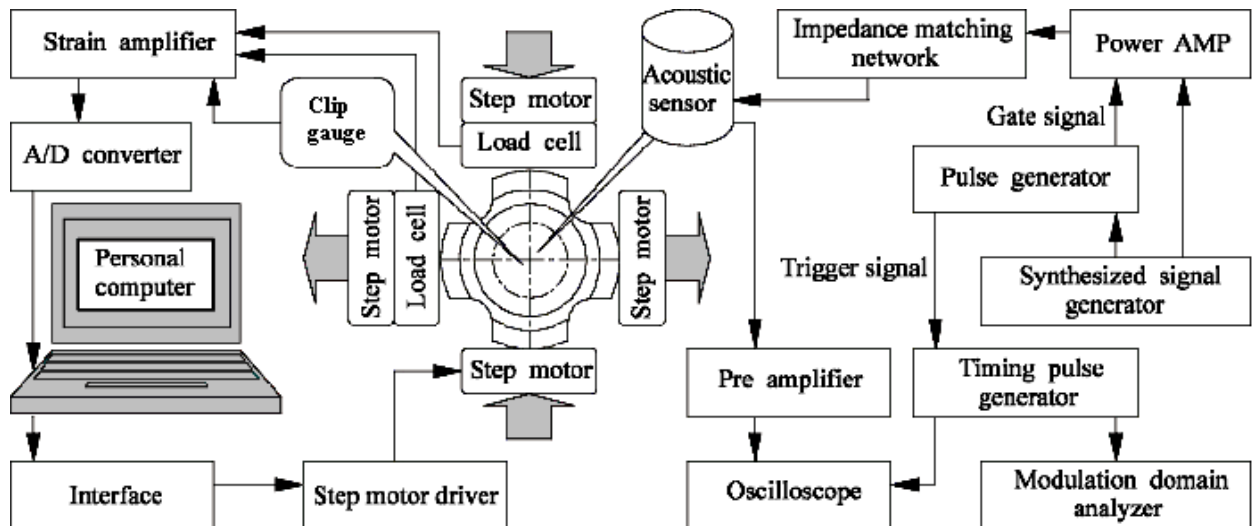


Fig.4 Block diagram of biaxial loading

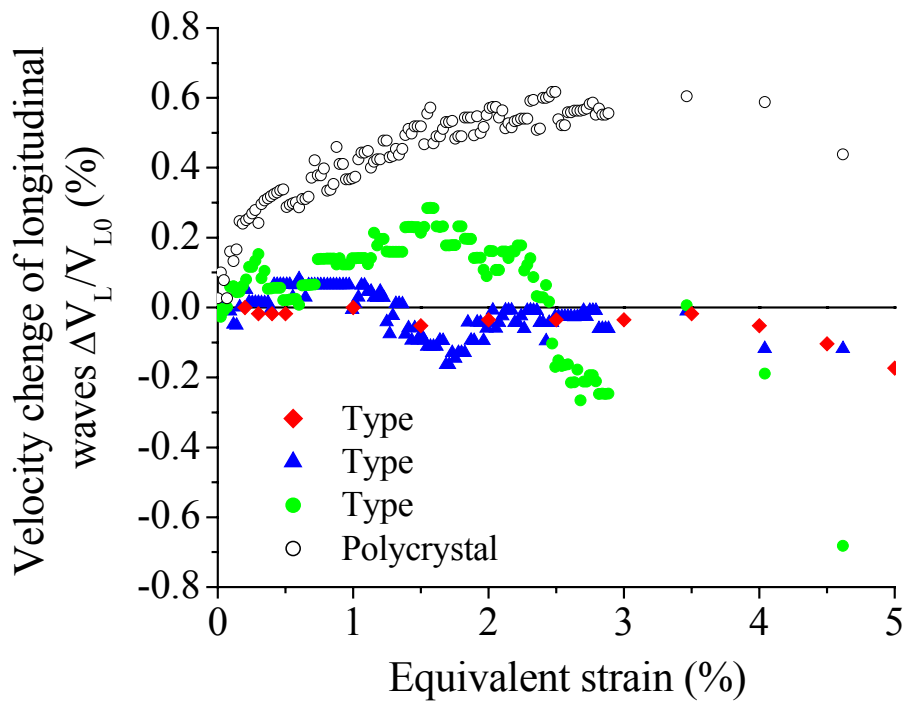


Fig.5 Comparison of experimental longitudinal wave velocity changes under pure shear state

Experimental Examination of Proposed Unified Criterion for Localized and Diffused Necking

Figure 6 shows the block diagram of experimental setup to measure onset strains of localized and diffused necking using laser speckle method and fractal dimensional analysis of speckle patterns. When the localized deformation occurs, the fractal dimension of the laser speckle pattern is saturated, therefore the onset strain at the localized or diffused necking can be found by fractal dimensional analysis of the laser speckle pattern. Figure 7 shows an example of changes of fractal dimension caused by plastic deformations in the several cases of proportional loading paths.

In Fig.8 FEM simulations regarding to the contour line of point defect amounts under several proportional loading paths are performed and compared with the experimental necking onset strains in Aluminum specimens measured by laser speckle method and fractal dimensional analysis of speckle patterns. The good agreement

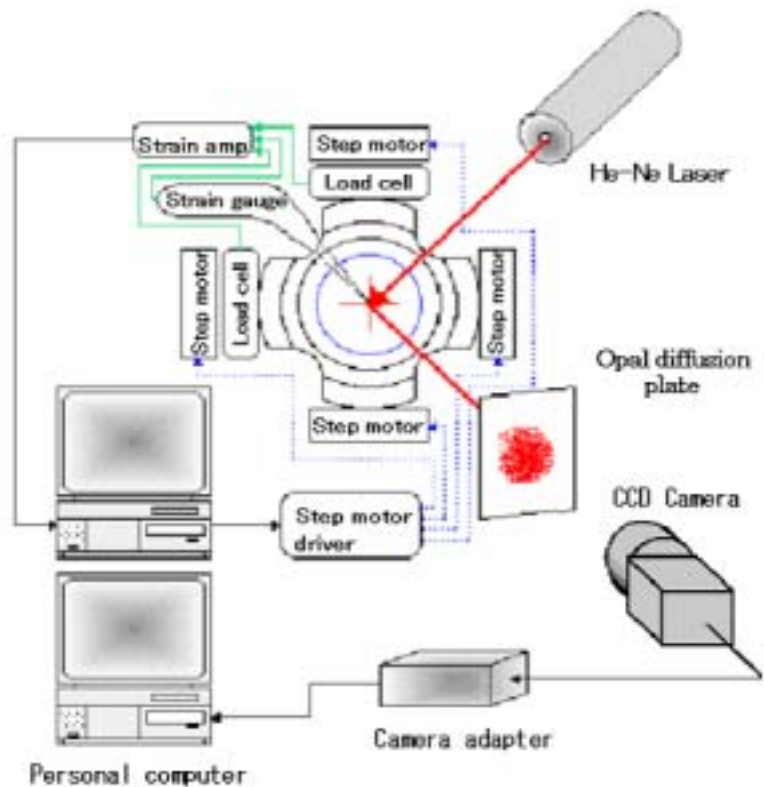


Fig. 6 Block diagram of laser speckle experimental setup

between the simulated and experimental results in Fig. 8 suggests that the proposed algorithm to calculate the amount of point defect defined by Eq. (3) has ability to be unified criterion for both localized and diffused necking.

To examine the correlation between point defect distributions and necking geometries, the examples of the point defect distribution in the cases of pure shear and biaxial tension states which are the representative localized and diffused necking, respectively, are compared in Figs. 9 and 10. As seen from Figs. 9 and 10 the area expansions of point defect in the biaxial tension case diffused widely, on the other hand in the pure shear case still remains locally.

Concluding Remarks

It is well known that the associative flow rule as the plastic constitutive equation has poor ability to analyze the deformation instability, ex. localized deformation or necking, and then the majority of researchers has adopted the corner theory as the plastic constitutive equation. One of authors proposed a kind of the plastic constitutive equation similar to the corner theory (cf. Stören and Rice [8]) to formulate the ultrasonic wave velocities in which the plastic strain rate is deviated from the normality of the yield surface by elastic stiffness degradation due to plastic deformation damage so called elasto-plastic coupling effect as pointed out by Il'iushin [8].

In this paper, via the experimental verification of the point defect dependence of the longitudinal wave velocity which is deduced to the elastic stiffness degradation due to plastic deformation and closely related to the deformation instability the proposed algorithm to calculate the amount of point defects is experimentally examined to be unified criterion for localized deformation or necking; the good agreement between the simulated and experimental onset strains of localized and diffused necking was obtained.

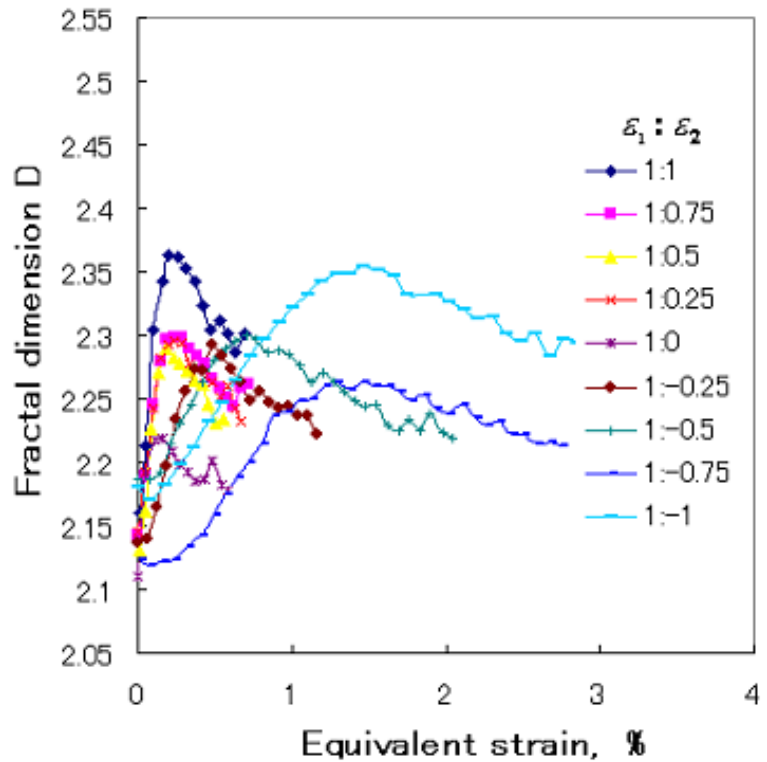


Fig. 7 Example of fractal dimension changes of laser speckle pattern on Aluminum specimens under proportional strain paths

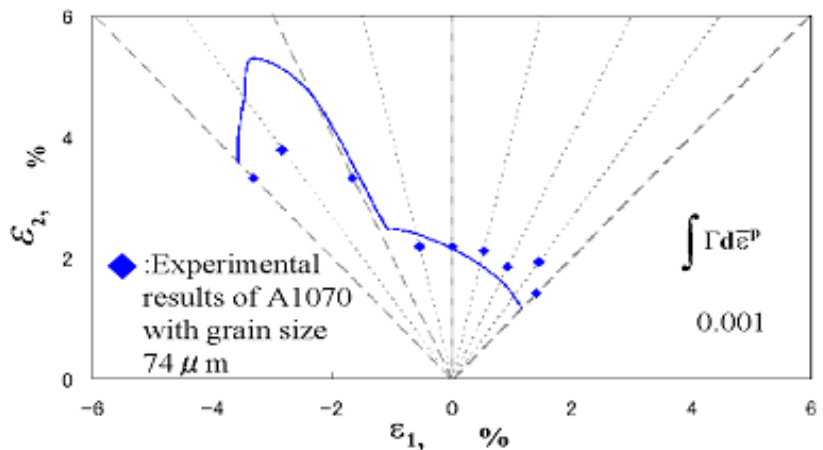


Fig.8 Comparison of localized deformation diagram between simulated result and experimental data of A1070 with grain size 74 μm

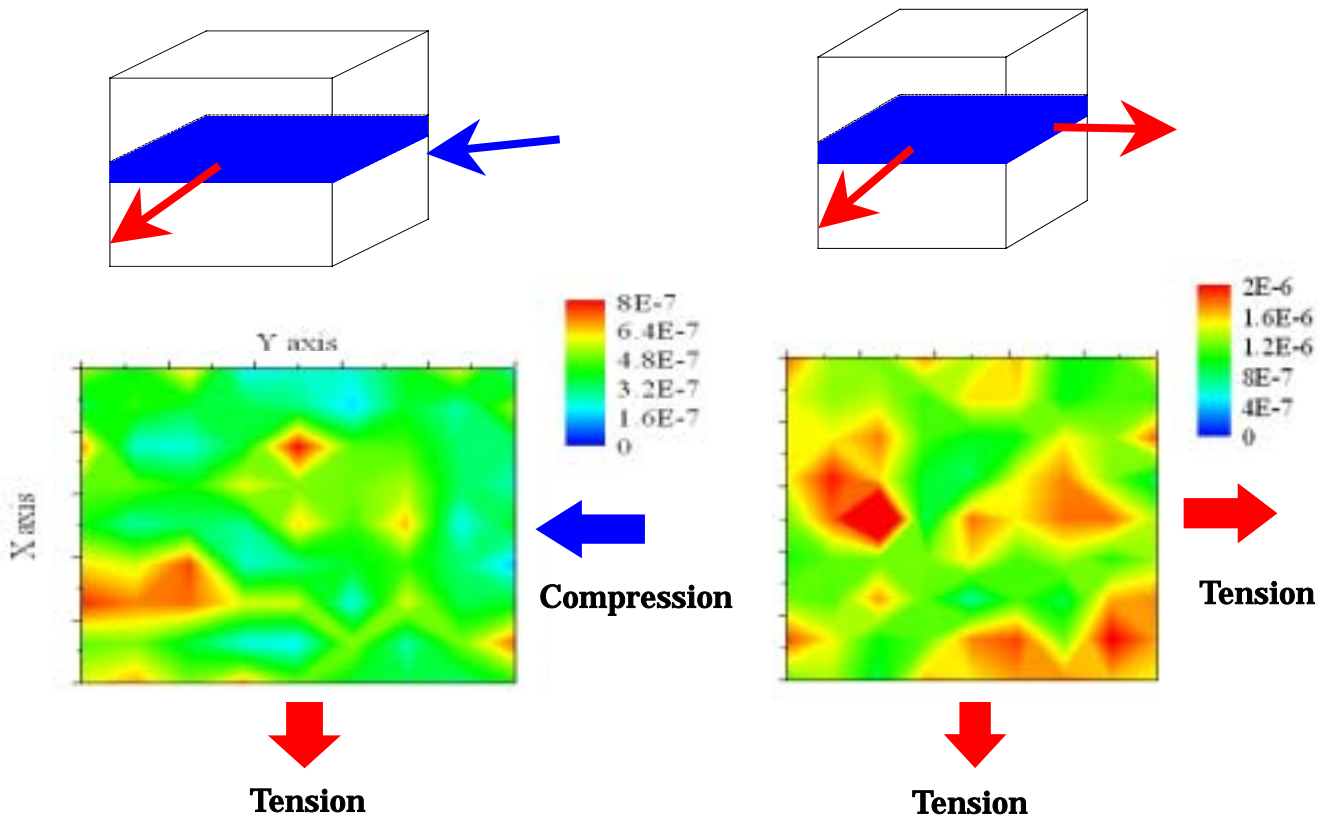


Fig. 9 Example of point defect distribution in the case of pure shear state as representative localized necking at 20% equivalent plastic strain

Fig. 10 Example of point defect distribution in the case of biaxial tension state as representative diffused necking at 20% equivalent plastic strain

References

- [1] M. Kobayashi: Tran. Jpn Soc. Mech. Eng. A48(1982), p.1072
- [2] M. Kobayashi: Int. J. Plasticity Vol. 3(1987), p. 1
- [3] M. Kobayashi: Int. J. Plasticity Vol. 14(1998), p. 511
- [4] M. Kobayashi, S. Tang, S. Miura, K. Iwabuchi, S. Oomori and H. Fujiki: Int. J. Plasticity Vol. 19(2003), p.771
- [5] M. Kobayashi. and S. Tang: J. Acoust. Soc. Am., Vol. 115(2004), p.637
- [6] H. Takahashi, H. Motohashi, M. Tokuda and T. Abe: Int. J. Plasticity Vol. 10(1994), p.63
- [7] H. Takahashi, T. Fujiwara and T. Nakagawa: Int. J. Plasticity Vol. 14(1998), p.489
- [8] S. Stören and J. R. Rice, J. Mech. Phys. Solids Vol. 23(1975),p.421
- [9] A. A. Il'iushin: PMM Vol. 24(1960), p.663